Equivalent Circuit Analysis of Harmonic Distortions in Photodiode

H. Jiang and P. K. L. Yu, *Senior Member, IEEE*

***Abstract*—We report a simple method to obtain a p-i-n photodiode's harmonic distortion levels at different frequencies from the microwave reflection coefficient S_{11} of the photodiode under dc illumination. This approach is based upon the tracking of the photodiode's microwave impedance with S_{11} at different incident optical powers before severe saturation occurs at low bias or at high optical power. The second-harmonic distortions measured from a waveguide photodiode agree closely with those predicted from the S_{11} data.**

***Index Terms*— Analog fiber-optic link, harmonic distortion, photodiode.**

I. Introduction

In ANALOG fiber-optic links, a p-i-n photodiode is commonly used at the receiver. The linearity of the photodiode is critical in the consideration of the overall link performance. In previous studies, nonlinear distortions of the p-i-n photodiode have been attributed mainly to the nonlinear transport induced by the space charge [1]–[3]. One-dimensional (1-D) numerical models that solve the Poisson equation and the carrier continuity equations under various operating conditions were developed to describe the nonlinear transport inside the device [2], [3].

Conventionally, the harmonic levels of the photodiode are measured by subjecting the photodiodes to heterodyned lasers with wavelength slightly offset to generate a RF tone. Alternatively, beat signals are generated at the photodiode using three separate optical beams RF-modulated at frequencies f_1, f_2 and f_3, respectively: the second-order intermodulation distortion signal at f_1+f_2, and the third-order intermodulation distortion at $f_3-(f_1+f_2)$ are measured [4].

In this work, we present and demonstrate a simple method to determine the p-i-n photodiode's harmonic distortion levels at different frequencies from the photodiode's microwave impedance variation at different optical powers. The microwave impedance is extracted from photodiode's microwave reflection coefficient (S_{11}). This method can predict the harmonic distortion levels at various incident optical powers before severe saturation occurs as a result of low bias or high optical power. We have experimentally tested this approach by comparing the measured second-harmonic signal of a waveguide photodiode with that predicted by an equivalent circuit model and parameters extracted from S_{11} data.

Manuscript received May 19, 1998; revised July 15, 1998. This work was supported in part by the Air Force Research Laboratory and in part by TRW.

The authors are with the Department of Electrical and Computer Engineering, University of California at San Diego, La Jolla, CA 92093-0407 USA.

Publisher Item Identifier S 1041-1135(98)07920-8.

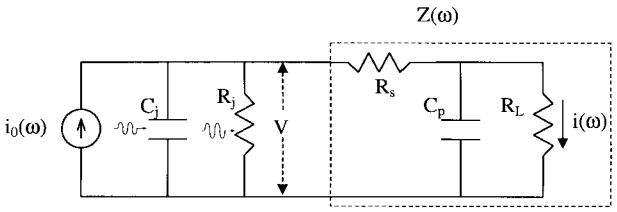

Fig. 1. An equivalent circuit of a p-i-n photodiode under illumination.

II. Theory

An equivalent circuit of the p-i-n photodiode is shown in Fig. 1 where $i_o(\omega)$ represents the photocurrent at ω inside the reverse-biased intrinsic region, C_j is the junction capacitance, R_j is the diode shunt junction resistance, C_p is the parasitic capacitance, R_s is the series resistance due to the contacts and the p and n regions of the diode, and R_L is the load resistor. For this circuit, the output current $i(\omega)$ can be expressed as $i(\omega)=i_o(\omega)\bullet H(\omega)$, where $H(\omega)$ is the transfer function of the circuit [5]. The form of $i(\omega)$ suggests that the harmonic distortion can manifest in $i_o(\omega)$ or $H(\omega)$, or both. The physical origin of the nonlinearity in $i_0(\omega)$ and $H(\omega)$ are attributed to the nonlinear carrier transport and the associated impedance changes induced by the optical input signal.

Previous work [1]–[3] on harmonic distortion of photodiode emphasized the analysis of nonlinear carrier transport, especially when the diode is under high power illumination. When the density of photogenerated electrons and holes reaches a level high enough to partially screen the biasing electric field which in turn gives rise to a nonuniform carrier velocity profile, the photodiode is already in severe saturation with high nonlinear distortion levels. However, the distortion can also rise in response to a change in the photodiode impedance even at a relatively low optical power.

Viallet *et al.* reported the increase of junction capacitance C_j of a planar p-i-n photodiode under optical illumination [6]. As can be seen from our work, a similar increase is observed in the waveguide p-i-n photodiode. The increase in C_j can be explained by an increase in the electric polarization due to an increase in photogenerated electron-hole pairs, whose density depends on the net electric field and optical illumination level. In general, both R_j and C_j change with optical illumination. For simplicity, we consider first the effect of C_j and assume it increases linearly with photocurrent:

$$C_j = C_{\rm dark} + I_{\rm dc}C' \tag{1}$$

where $C_{\rm dark}$ is the dark capacitance of the junction, $I_{\rm dc}$ is the dc photocurrent, and C' is defined as the differential

capacitance with respect to the photocurrent. In the equivalent circuit of Fig. 1, the equation for the voltage V across the current source (from which we obtain the voltage across the load) is

$$\frac{d}{dt}\{(C_{jo}+i_o e^{j\omega t}C')V\}+\frac{V}{R_{jo}}+\frac{V}{Z(\omega)}=i_o e^{j\omega t} \tag{2}$$

where C_{jo} and R_{jo} are the junction capacitance and resistance at a given $I_{\rm dc}$, and $Z(\omega)$ is the equivalent impedance of C_p, R_s, and R_L given by

$$Z(\omega)=R_s+\frac{1}{\left(\dfrac{1}{R_L}+j\omega C_p\right)}. \tag{3}$$

V can be expressed in a harmonic series of $V_1e^{j\omega t}+V_2e^{j2\omega t}+V_3e^{j3\omega t}+\cdots$, where V_1, V_2, and so on can be obtained from

$$V_1=\frac{i_o}{\dfrac{1}{R_{jo}}+j\omega C_{jo}+\dfrac{1}{Z(\omega)}} \tag{4}$$

$$V_2=-\frac{2j\omega C' i_o}{\dfrac{1}{R_{jo}}+2j\omega C_{jo}+\dfrac{1}{Z(2\omega)}}V_1. \tag{5}$$

The above analysis suggests certain relationships between the photodiode's harmonic levels and the microwave impedance. For instance, a relatively large change in C_j can enhance harmonic levels, while the fundamental power remains largely unchanged. This analysis shows that harmonic powers are subject to a similar *RC* frequency rolloff as the fundamental signal. At frequencies well below the rolloff, harmonic powers are proportional to ω^2 provided that the variation of C_j dominates, which agrees qualitatively with experimental observation [1]. The above assumes that the photodiode is not in severe saturation and that C_{jo} increases gradually from its dark value. Under low illumination R_{jo} does not decrease substantially from the dark resistance, and the second-harmonic distortion level is not much affected by changes in R_j, as R_j is usually much larger than R_L. To describe higher order distortions and the high optical power situation where carrier screening can be important, we have to include effects of a changing R_j in the analysis.

III. Photodiode Impedance and Harmonic Measurements

We measure the S_{11} of an InGaAs–InP photodiode and use the equivalent circuit of Fig. 1 to analyze the impedance. They are obtained as a function of the optical input level and the bias voltage. For the S_{11} measurement, a one-port microwave calibration of the vector network analyzer (HP 8703), along with the microwave cable and microwave probe (Picoprobe, 40A-GSG-200-DP) is performed using a standard impedance substrate (Cascade LRM ISS GSG). A waveguide p-i-n photodetector integrated with a CPW microwave transmission line is used in this experiment [7]. The particular device used has a small signal 3-dBe bandwidth of 20 GHz and a responsivity of 0.35 A/W. In the optical set-up, a polarization insensitive, variable optical attenuator and a fiber coupler with a 10 : 1 splitting ratio are inserted in the fiber link between a CW Nd : YAG laser ($\lambda = 1.319$ μm) and the photodiode for adjusting the input power. The smaller output power port of the coupler is connected to an optical power meter. In the S_{11} measurement the input RF is at -10 dBm and is ranged from 200 MHz to 20 GHz in frequency, the photodiode is reverse-biased at 3 and 5 V.

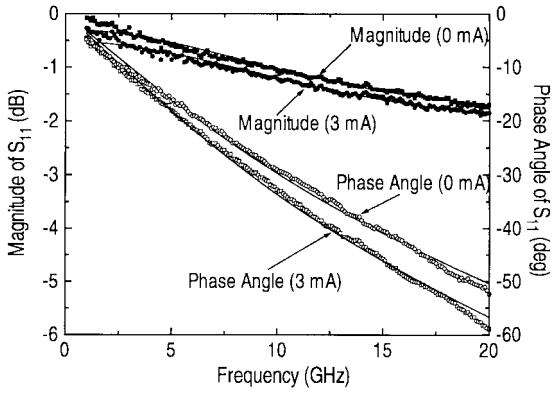

Fig. 2. The measured (dotted) S_{11}'s at 0 and 3 mA photocurrent. Solid curves correspond to the best fitting of the measured data.

TABLE I
Samples of Junction Capacitance and Resistance of the Waveguide Photodiode (with 4 × 35 μm^2 Junction Area and 0.45-μm-Thick Intrinsic Region) Obtained from S_{11} Data

Photocurrent (mA)	- 3V bias		- 5 V bias	
	C_j (fF)	R_j (kΩ)	C_j (fF)	R_j (kΩ)
0	41.0	11.922	41.0	12.621
1	42.0	2.073	41.5	12.650
2	42.8	1.004	42.4	11.848
3	44.0	0.975	43.6	11.424

We also evaluate nonlinear distortion levels of the same photodiode. We measure simultaneously the RF fundamental and the second-harmonic signals in the 0–1.5-mA photocurrent range at various frequencies, and under different biases, using two temperature-tuned 1.319-μm Nd : YAG lasers to provide a RF tone in a heterodyne configuration. In the setup, the output of one of the lasers is coupled via a polarization controller to a 3-dB coupler along with the other laser output. One output of the coupler feeds to another photodetector whose output is used as the feedback reference signal to the laser controller to stabilize the frequency separation of the lasers. The other output of the coupler feeds via a variable attenuator to the device under test. The setup provides a maximum optical power of 3 mW (limited by the lasers) with a RF tone at 100% modulation depth in the 0.1–1-GHz frequency range. The polarization controller ensures the same polarization of the lasers as the frequency is varied. Measurements are done at different photocurrent levels with 260-, 400-, 500-, 600-, 700-MHz frequency separations between the lasers and at reverse-biases of 3 and 5 V.

IV. Results and Discussions

Fig. 2 shows measured S_{11} of the photodiode at -5-V bias and at 0 and 3-mA photocurrent. C_j, R_j, R_s, and C_p values

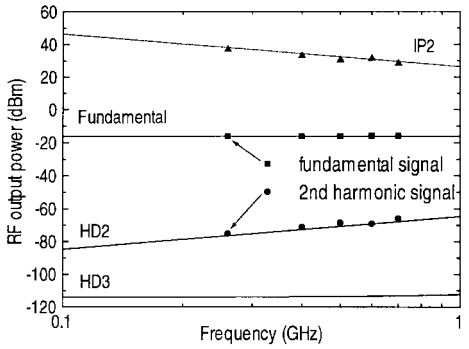

Fig. 3. Fundamental and harmonic signals at -5 V versus frequency. The dots are measured results and the solid curves represent predictions from the analysis using S_{11} data. The predicted and extracted output referenced $IP2$ are included. $I_{ph} = 1$ mA.

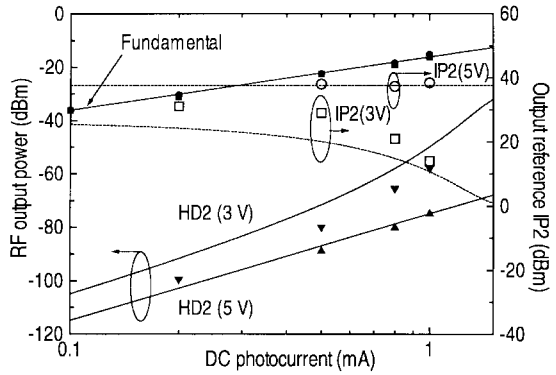

Fig. 4. Fundamental and second-harmonic signals, at 260 MHz and at -3 (■, ▼) and -5 V (•, ▲), respectively, versus photocurrent. The dots and solid curves are the measured and theoretical results, respectively. The predicted (dash line) and extracted output referenced $IP2$ at -3 (□) and -5 V (○) are included.

are obtained from best curve fitting to S_{11}'s. R_s and C_p are 110 Ω and 0.07 pF, respectively, in all cases. Table I shows some of the C_j's and R_j's obtained. It is seen that C_j increases and R_j decreases with photocurrent.

At -5 V, the R_j of the photodiode remains at ∼12 kΩ up to 3 mA of photocurrent. Since $R_j \gg R_L$, its small variation has little effect on the second-harmonic level. At low photocurrent, the C' is ∼0.8 fF/mA. With these we calculate the fundamental signal and second-harmonic distortion at -5-V and 1-mA photocurrent at unity modulation index, based on (3)–(5). The resulting fundamental and second-harmonic distortion signals for frequencies ranging from 0.1 to 1 GHz are depicted in Fig. 3. We also show the results for predicted third-harmonic distortion based upon changes in both C_j and R_j. In the same graph, we also show the fundamental and second-harmonic distortion results using heterodyned lasers at the same modulation index ($m = 1$). A close agreement between calculation and measurement is obtained at -5 V.

At a given photocurrent level, a lower bias results in a smaller applied electric field and less effective sweeping of the carriers out of the intrinsic region. This, together with a larger photogenerated carrier density, can lower the junction resistance. Thus as the photocurrent increases, R_j is more reduced when biased at -3 V than at -5 V. Fig. 4 depicts the predicted fundamental and second-harmonic distortions of the photodiode biased at -3 and -5 V at different photocurrent and at 260 MHz operating frequency, based upon changes of R_j and C_j. However, a closer agreement between calculation and measurement is obtained at -5 V. The frequency dependence of the distortions reflects mainly the assumed coupling between the photocurrent and the change in capacitance (and junction resistance).

For analog link applications, the two-tone intermodulation distortions of the link are of much importance. The output referenced second order intermod intercept ($IP2$) is 6 dB lower than the second order harmonic intercept (more exactly, $IP2\,(\text{dBm}) = 2P_1\,(\text{dBm}) - P_2\,(\text{dBm}) - 6$ dB, where P_1 and P_2 are the fundamental and second-harmonic power, respectively). The predicted $IP2$ curves and the extracted $IP2$ from measured data are included in Figs. 3 and 4.

The above analysis can be useful for examining various circuit elements' influence on harmonic levels. For instance, the photodiode used has a relatively high series resistance R_s and the analysis indicates that a more than 9-dB reduction in the second-harmonic distortion can result if R_s is reduced from 110 to 10 Ω.

V. Conclusion

We have used an equivalent circuit model to calculate harmonic distortions of a p-i-n photodiode from the measured S_{11} under dc optical illumination. The method can be used to predict the $IP2$ of the photodiode under various operation conditions. It may be useful for evaluating the photodiode before packaging.

Acknowledgment

The authors would like to thank G. L. Li at the University of California at San Diego and Dr. T. Vang at TRW for helpful discussions.

References

[1] R. R. Hayes and D. L. Persechini, "Nonlinearity of p-i-n photodetectors," *IEEE Photon. Technol. Lett.*, vol. 5, pp. 70–72, Jan. 1993.
[2] K. J. Williams, R. D. Exman, and M. Dagenais, "Nonlinearities in p-i-n microwave photodetectors," *J. Lightwave Technol.*, vol. 14, pp. 84–96, 1996.
[3] J. Harari, G. Jin, J. P. Vilcot, and D. Decoster, "Theoretical study of p-i-n photodetectors' power limitations from 2.5 to 60 GHz," *IEEE Trans. Microwave Theory Tech.*, vol. 45, pp. 4332–4336, Aug. 1997.
[4] T. Ozeki and E. H. Hara, "Measurement of nonlinear distortion in photodiodes," *Electron. Lett.*, vol. 12, pp. 80–81, 1976.
[5] P. Bhattacharya, *Semiconductor Optoelectronic Devices.* Englewood Cliffs, NJ: Prentice-Hall, 1994, p. 350.
[6] J. E. Viallet, S. Mottet, L. L. Juerou, and C. Boisrobert, "Photodiode for coherent detection: Modeling and experimental results," *J. Phys. C4*, vol. 49, pp. 321–324, Sept. 1988.
[7] A. R. Williams, A. L. Kellner, X. S. Jiang, and P. K. L. Yu, "InGaAs/InP waveguide photodetector with high saturation intensity," *Electron. Lett.*, vol. 28, no. 24, pp. 2258–2259, 1992.